Numerical simulation of a rotating Bose Einstein condensate

Ionut Danaila

Laboratoire Jacques-Louis Lions, Université Pierre et Marie Curie, 175 rue du Chevaleret, 75013 Paris.

Mots-clefs : finite differences, compact schemes, Bose-Einstein condensate, vortex

Abstract

A high order finite difference method is used to numerically investigate the three-dimensional structure of vortices appearing in rotating Bose-Einstein condensates confined in a harmonic trap. Single vortex configurations recently observed in experiments [6] are described in detail. Multiple vortex configurations are also considered.

1 Introduction

Several experimental groups have produced vortices in Bose Einstein condensates (BEC) by a rotation of the trapping potential [1, 5, 3, 2, 4, 6]. The number and shape of vortices depend on the rotational frequency and the geometry of the trap. For an elongated trap with a single vortex, experimental [2, 3, 6] and theoretical [7, 8] evidence was provided to prove that the vortex line is not straight along the axis of rotation, but bending. The vortex displays therefore a U shape. Recently, more complicated configurations (S) were observed in experiments [6].

Bending (or U) vortex is a topic that has been receiving a great deal of attention from people conducting numerical simulations. Most of the numerical studies use minimization algorithms [9, 10] to compute local minima of the Gross Pitaevskii energy. While the U vortex was described in detail, multiple vortex configurations were briefly addressed in these studies, providing either a short description of the three-dimensional topology [9], or the evolution of the energy and angular momentum [10].

In this paper, motivated by the recent experiments at the ENS [6], a high order finite difference method is proposed to numerically investigate the three-dimensional shape of vortex configurations in a prolate rotating condensate. Our aim is to understand the various vortex configurations observed ion experiments: U vortices but also S. Solutions with up to 4 vortices are also considered.

2 Mathematical model

We consider a pure BEC of N atoms confined in a harmonic trapping potential rotating along the z axis at angular velocity Ω. The equilibrium of the system corresponds to local minima of the Gross-Pitaevskii energy in the rotating frame

$$\mathcal{E}_{3D}(\phi) = \int_{\mathcal{D}} \frac{\hbar^2}{2m} |\nabla\phi|^2 + \hbar\boldsymbol{\Omega} \cdot (i\phi, \nabla\phi \times \mathbf{x}) + \frac{m}{2} \sum_{\alpha=x,y,z} \omega_\alpha^2 r_\alpha^2 |\phi|^2 + \frac{N}{2} g_{3D}|\phi|^4, \qquad (1)$$

where $g_{3D} = 4\pi\hbar^2 a/m$ and the wave function ϕ is normalized to unity $\int_{\mathcal{D}} |\phi|^2 = 1$. Here, for any complex quantities u and v and their complex conjugates $\bar{u}$ and $\bar{v}$, $(u,v) = (u\bar{v} + \bar{u}v)/2$.

For numerical applications, it is more convenient to use the dimensionless energy introduced in [7]

$$E_{3D}(u) = \int_{\mathcal{D}} \frac{1}{2}|\nabla u|^2 + \tilde{\mathbf{\Omega}} \cdot (iu, \nabla u \times \mathbf{r}) - \frac{1}{2\varepsilon^2}\left(\rho_0 - (x^2 + \alpha^2 y^2 + \beta^2 z^2)\right)|u|^2 + \frac{1}{4\varepsilon^2}|u|^4 , \quad (2)$$

where the variables are scaled as following :

$$d = \left(\frac{\hbar}{m\omega_x}\right)^{1/2}, \ \varepsilon = \left(\frac{d}{8\pi N a}\right)^{2/5}, \ R = \frac{d}{\sqrt{\varepsilon}},$$

$$\mathbf{r} = \mathbf{x}/R, \ u(\mathbf{r}) = R^{3/2}\phi(\mathbf{x}),$$

$$\tilde{\Omega} = \Omega/(\varepsilon\omega_x), \ \alpha = \omega_y/\omega_x, \ \beta = \omega_z/\omega_x.$$

The constant ρ_0 does not affect minimizers of (2), since it multiplies $|u|^2$ and $\int_{\mathcal{D}} |u|^2 = 1$. For small ε, considering the Thomas-Fermi approximation $\rho_{\mathrm{TF}}(\mathbf{r}) = \rho_0 - (x^2 + \alpha^2 y^2 + \beta^2 z^2)$ for $|u|^2$, we obtain a straightforward definition of ρ_0 and the domain $\mathcal{D}$:

$$\rho_0^{5/2} = 15\alpha\beta/8, \quad \mathcal{D} = \{\rho_{\mathrm{TF}}(\mathbf{r}) \geq 0\} .$$

Let us finally remind that the GP energy (2) can be written as

$$E_{3D}(u) = H(u) - \tilde{\mathbf{\Omega}} L_z(u), \quad (3)$$

with the angular momentum defined as

$$L_z(u) = i \int_{\mathcal{D}} \bar{u}\left(y\frac{\partial u}{\partial x} - x\frac{\partial u}{\partial y}\right). \quad (4)$$

3 Numerical method

In the present study we compute critical points of $E_{3D}(u)$ by solving the norm-preserving imaginary time propagation of the corresponding equation:

$$\frac{\partial u}{\partial t} - \frac{1}{2}\Delta u + i(\tilde{\mathbf{\Omega}} \times \mathbf{r}).\nabla u = \frac{1}{2\varepsilon^2}u(\rho_{\mathrm{TF}} - |u|^2) + \mu_\varepsilon u, \quad (5)$$

with $u = 0$ on $\partial\mathcal{D}$ and μ_ε the Lagrange multiplier for the norm constraint $\int_{\mathcal{D}} |u|^2 = 1$:

$$\mu_\varepsilon = \int_{\mathcal{D}}\left\{\frac{1}{2}|\nabla u|^2 - \frac{1}{2\varepsilon^2}(\rho_{\mathrm{TF}} - |u|^2)|u|^2\right\} - \tilde{\mathbf{\Omega}} L_z. \quad (6)$$

A hybrid 3 steps Runge-Kutta-Crank-Nicolson scheme [12] is used to advance the equation in time:

$$\frac{u_{l+1} - u_l}{\Delta t} = a_l\mathcal{H}_l + b_l\mathcal{H}_{l-1} + c_l\Delta\left(\frac{u_{l+1} + u_l}{2}\right), \quad (7)$$

where $\mathcal{H}$ contains the remaining non-linear terms. The corresponding constants for every step $(l = 1, 2, 3)$ are :

$$\begin{array}{lll} a_1 = 8/15, & a_2 = 5/12, & a_3 = 3/4, \\ b_1 = 0, & b_2 = -17/60, & b_3 = -5/12, \\ c_1 = 8/15, & c_2 = 2/15, & c_3 = 1/3. \end{array}$$

The resulting semi-implicit scheme is second order time accurate and allows reasonably large time steps, making it appropriate for long time integration. The large sparse matrix linear systems resulting from the implicit terms are solved by an alternating direction implicit (ADI) factorization technique.

For the spatial discretization we use finite differences on a Cartesian uniform mesh with periodic boundary conditions in all directions. To accurately resolve sharp gradients of the variable in presence of vortices, low numerical dissipation and very accurate schemes are required for the spatial derivatives. A sixth-order compact finite difference scheme [13] with spectral-like resolution was chosen to this end. The first and second derivatives at the grid point i are written as :

$$\frac{1}{3}u'_{i-1} + u'_i + \frac{1}{3}u'_{i+1} = \frac{14}{9}\frac{u_{i+1} - u_{i-1}}{2h} + \frac{1}{9}\frac{u_{i+2} - u_{i-2}}{4h},$$

$$\frac{2}{11}u''_{i-1} + u''_i + \frac{2}{11}u''_{i+1} = \frac{12}{11}\frac{u_{i+1} - 2u_i + u_{i-1}}{h^2} + \frac{3}{11}\frac{u_{i+2} - 2u_i + u_{i-2}}{4h^2},$$

where h is the step of the space discretization. The values of the derivatives at all the grid points are computed by solving a tridiagonal matrix linear system, which provides spectral-like behavior of the finite difference scheme.

4   Physical and numerical parameters

The values of constants in (5) are set to $\varepsilon = 0.02$, $\alpha = 1.06$, $\beta = 0.067$, corresponding to the experiments of the ENS group [10, 3]. The rotation frequency Ω will be varied from 0 to the maximum value of $0.9\omega_x$, for which no deformation of the condensate has to be taken into account.

Equation (5) is propagated in imaginary time until the evolution of the energy (2) displays a long time lasting plateau corresponding to a gradient smaller than 10^{-6}. For the considered range of Ω, the numerical domain is fixed to an elongated box $(x, y, z) \in [-0.6, 0.6] \times [-0.6, 0.6] \times [-8.5, 8.5]$. A refined grid using $72 \times 72 \times 510$ nodes was employed, which was sufficient to achieve grid-independence for all considered numerical experiments.

Different initial conditions were used in order to trigger single or multiple vortex configurations and follow the corresponding branches by continuity. The simplest initial condition assumes a steady-state solution $u(x, y, z) = \sqrt{\rho_{\mathrm{TF}}(x, y, z)}$ and is useful to study vortex-free configurations and their degeneracy into multiple vortex configurations when increasing the value of Ω. Initial conditions with vortices are obtained by superimposing to the steady-state a simplified model for the vortex.
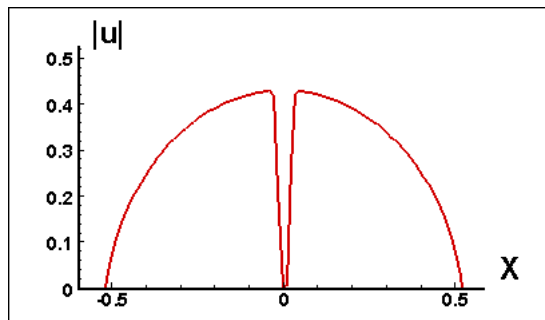
Figure 1: Density profile along a line crossing a centered vortex.

For example, an initial condition with a centered straight vortex of radius ε is obtained by imposing

$$u(x, y, z) = \sqrt{\rho_{\text{TF}}} \cdot u_\varepsilon \cdot exp(i\varphi), \qquad (8)$$

$$u_\varepsilon = \sqrt{0.5 \left\{ 1 + tanh \left[\frac{4}{\varepsilon} (r - \varepsilon) \right] \right\}},$$

where (r, φ) are the polar coordinates in the (x, y) plane and the density profile u_ε is shown on figure 1.

The 3D shape of the vortex can be easily modified by shifting the center r_0 of the vortex in successive (x, y) planes - for instant, to obtain a planar S shape vortex, the following function can be used:

$$r_0(z) = \begin{cases} -1 + tanh \left[\alpha_v \left(1 + \frac{z}{\beta_v} \right) \right] \Big/ tanh(\alpha_v), & z < 0 \\ 1 + tanh \left[\alpha_v \left(-1 + \frac{z}{\beta_v} \right) \right] \Big/ tanh(\alpha_v), & z \geq 0 \end{cases}$$

The constants α_v, β_v control, respectively, the curvature and the height of the vortex.

5   Numerical results

The U vortex was numerically obtained by starting the simulation from an initial condition containing a straight vortex away from the z axis. For a relatively large value of the rotation frequency ($\Omega = 0.58\omega_x$) the final steady state (i.e. the local minimum of the GP energy) displays a planar U shape with a straight central part on the z axis and and an outer part reaching the condensate boundary perpendicularly. We then increased or decreased Ω by small steps ($\delta\Omega = 0.04\omega_x$) and continuously followed this solution branch (for a given Ω, the run starts from the initial condition provided by the steady state obtained for $\Omega \pm \delta\Omega$).
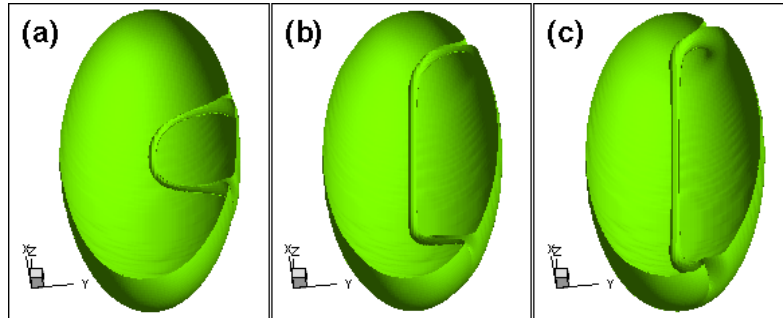
Figure 2: Single U vortex configurations for $\Omega/\omega_x = 0.42$ (a), 0.58 (b), 0.78 (c).

The U vortex exists for the range $\Omega/\omega_x \in [0.42, 0.86]$. At the lower bound, the U vortex disappears and a vortex-free configuration is obtained, while at the higher bound the U vortex degenerate in a three-vortex configuration (described later). When Ω increases, the central straight part gets longer (fig. 2), but the vortex always displays a small bent region at its ends. In the attempt to get a completely straight vortex, we considered an initial condition with a straight vortex, centered on the z axis. It turned out that the vortex becomes bent for $\Omega < 0.8\omega_x$, recovering the previous configurations. The straight vortex (figure 3) stays stable for $\Omega > 0.8\omega_x$, which is in agreement with the result of [8] where the local stability of the straight vortex for Ω large was proved.
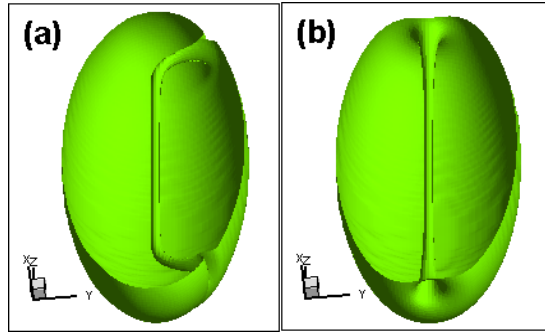
Figure 3: Stable configurations obtained from an initial condition with a straight vortex configurations for $\Omega/\omega_x = 0.6$(a), 0.8 (b).

Motivated by the experiments of [6], we compute new critical points of the energy, which are S configurations (see figure 4). S vortices were numerically obtained from initial conditions generated as described in §4. Several numerical experiments were performed. First of all, we checked that the final steady state for a given Ω is always the same (different initial planar S shapes evolved to the same final configuration). We could also check that non planar S configurations with an angle between the branches different from 90 degrees, do not exist.
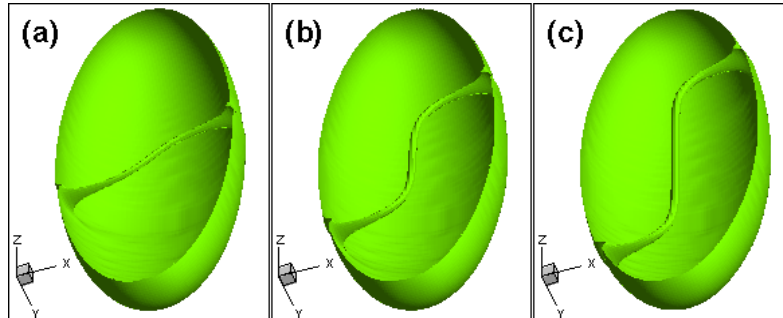
Figure 4: Single S vortex configuration for $\Omega/\omega_x = 0.38$ (a), 0.44 (b), 0.48 (c).

Multiple vortex configurations are obtained based upon different numerical strategies. The first one is to start the computation from a vortex-free steady state obtained for low and to abruptly increase Ω to a very hight value - multiple vortices are thus obtained. The second strategy is to generate an initial condition with vortices artificially *planted* (the advantage being the control of the shape and initial arrangement of the vortices).
Both techniques were used to follow solution branches with two, three or four vortices in the condensate. Further details about these configurations can be found in [14].

6   Conclusion

We have studied the numerical solutions of the Gross Pitaevskii equations in the framework of the ENS experiment. We have observed S and U vortices and multiple vortex configurations. Spectral-like finite difference scheme proved to be very effective in accurately capture the three-dimensional structure of vortices.

Références

[1] M.R.Matthews et al. Phys. Rev. Lett., **83**, 2498 (1999).

[2] K. Madison, F. Chevy, V. Bretin and J. Dalibard, Phys. Rev. Lett., **84**, 806 (2000).

[3] K. Madison, F. Chevy, W. Wohlleben and J. Dalibard, J. Mod. Opt., **47**, 2715 (2000).

[4] C. Raman, J. R. Abo-Shaeer, J. M. Vogels, K. Xu, and W. Ketterle Phys. Rev. Lett. **87**, 210402 (2001).

[5] J. R. Abo-Shaeer , C. Raman, J. M. Vogels , and W. Ketterle, Science **292**, 476 (2001).

[6] P. Rosenbuch, V. Bretin and J. Dalibard, Phys. Rev. Lett. **89**, 200403 (2002)

[7] A. Aftalion and T. Riviere, Phys. Rev. A **64**, 043611 (2001).

[8] A. Aftalion and R.L. Jerrard, Phys. Rev. A **66**, 023611 (2002).

[9] J. J. García-Ripoll and V. M. Perez-García, Phys. Rev. A **63**, 041603(R) (2001), Phys. Rev. A **64**, 053611 (2001).

[10] M. Modugno, L. Pricoupenko and Y. Castin, cond-mat/0203597.

[11] D.L. Feder and C.L. Clark Phys. Rev. Lett. 87, 190401 (2001).

[12] P. Orlandi, *Fluid Flow Phenomena*, Kluwer Academic Publishers (1999).

[13] S. K. Lele, J. Comp. Physics, **103**, 16 (1992).

[14] A. Aftalion, I. Danaila, cond-mat/0303416.